Research Square

Preprints are preliminary reports that have not undergone peer review.
They should not be considered conclusive, used to inform clinical practice,
or referenced by the media as validated information.

Hourly Clean Electricity Tracing and Masked Computation Support Enterprise Carbon Certification

Lingyu Chen
State Grid Sichuan Electric Power Research Institute
Yang Wei
State Grid Sichuan Electric Power Research Institute
Xiangxi Duan
State Grid Sichuan Electric Power Company
Hongli Liu
State Grid Sichuan Electric Power Research Institute
Han Zhang
State Grid Sichuan Electric Power Research Institute
Yumin Chen
State Grid Sichuan Electric Power Research Institute
Junhua Zhao
Chinese University of Hong Kong, Shenzhen
Tianze Yu
tianzeyu@link.cuhk.edu.cn

Chinese University of Hong Kong, Shenzhen

Article

Keywords:

Posted Date: November 20th, 2026

DOI: https://doi.org/10.21203/rs.3.rs-11499776/v1

License: This work is licensed under a Creative Commons Attribution 4.0 International License.
Read Full License

Additional Declarations: No competing interests reported.

Hourly Clean Electricity Tracing and Masked Computation Support Enterprise Carbon Certification

Lingyu Chen[1,2], Yang Wei[1,2], Xiangxi Duan[3], Hongli Liu[1,2], Han Zhang[1,2], Yumin Chen[1,2], Junhua Zhao[4], Tianze Yu[4*]

[1]State Grid Sichuan Electric Power Research Institute, Chengdu, 610059, China.
[2]Power System Security and Operation Key Laboratory of Sichuan Province, Chengdu, 610059, China.
[3]State Grid Sichuan Electric Power Company, Chengdu, 610041, China.
[4]The Chinese University of Hong Kong, Shenzhen, Shenzhen, China.

*Corresponding author(s). E-mail(s): tianzeyu@link.cuhk.edu.cn;

Abstract

Annual and regional emission factors obscure hourly and nodal variation in clean electricity availability. We developed a consumer-side carbon accounting workflow that combines hydropower dispatch, proportional-sharing electricity tracing and masked certification. In a modified IEEE 39-bus system, nodal clean electricity fractions ranged from 2.95 percent to approximately 100 percent, while three constructed industrial consumers had period-total fractions of 1.96–23.70 percent. A fixed Gaussian mask was shared among trustees and removed before release; a smaller hourly perturbation remained. Across 100 Monte Carlo runs, the released estimates had a mean absolute error of 2.200 MW and a period-total absolute error of 36.08 MWh, compared with 9.272 MW and 240.78 MWh for the tested local-noise baseline. The hybrid scheme also had a 49.24 percent mean absolute percentage error and a 9.33 percent clipping rate. These results support finer spatial attribution and lower absolute error under the selected settings, but do not establish a formal differential-privacy guarantee.

Keywords: Consumer-side carbon emission certification, Clean electricity tracing, Masked certification, Hydropower economic dispatch, Secret sharing, Fine-grained carbon accounting

1 Introduction

Driven by power-sector decarbonization, green electricity trading, and corporate carbon disclosure requirements, consumer-side carbon emission accounting has become increasingly important for evaluating the actual low-carbon performance of electricity users [1]. Electricity generation remains a major source of global carbon dioxide emissions, while electricity consumption is the key interface through which enterprises report indirect emissions and demonstrate clean energy use [2, 3]. However, conventional electricity-related carbon accounting methods commonly rely on annual or regional average emission factors, which cannot accurately capture the temporal variation of clean electricity supply or its mismatch with user demand. Recent studies and 24/7 carbon-free energy initiatives have therefore emphasized more granular electricity matching and hourly carbon accounting [4, 5]. These developments highlight

the need for a consumer-side carbon certification method that links clean electricity tracing with fine-grained carbon emission accounting.

Existing studies have investigated electricity-related carbon accounting from several perspectives. For example, a recent review systematically examined carbon accounting methods and measurement technologies for thermal power plants [6]. Scope 2 accounting frameworks provide location-based and market-based methods for reporting purchased electricity emissions, but they are mainly designed for inventory disclosure rather than for tracing the hourly clean electricity actually consumed by each enterprise [3, 4]. Power flow tracing and carbon emission flow methods further allocate generation or emission responsibilities through network-based models [7, 8]. Nevertheless, these methods are usually developed at the system, regional, or nodal level, and do not directly generate enterprise-level estimates that combine hourly clean electricity and carbon emissions. In addition, conventional green electricity claims often rely on volumetric certificate matching, which may conceal temporal mismatches between clean electricity generation and user demand [9, 10]. Therefore, existing methods remain insufficient for hourly, enterprise-level accounting with controlled disclosure.

In hydropower-dominated power systems, clean electricity supply is not a static attribute determined only by installed capacity. Reservoir hydropower can provide low-carbon generation and substantial operational flexibility, but its hourly output is constrained by water availability, reservoir balance, cascade coordination, unit operating limits, and system economic dispatch [11, 12]. This makes clean electricity attribution more complex than a simple proportional allocation based on annual renewable generation. Although abundant hydropower resources may increase the overall clean electricity share of the system, the clean electricity available to a specific consumer at a specific hour still depends on the dispatch schedule, load level, network power-flow allocation, and the coordination between hydropower and other generation resources [7, 8]. Consequently, enterprises with the same total electricity consumption may have different clean electricity consumption ratios and carbon emission responsibilities if their load profiles are distributed differently over time [4]. Therefore, enterprise-side clean electricity attribution should be linked to the hourly dispatch process of hydropower-dominated systems, providing an operational basis for subsequent carbon accounting.

Although hourly clean electricity tracing provides a more accurate basis for enterprise-side carbon accounting, it also introduces new privacy and trust challenges. Enterprise electricity consumption profiles may reveal sensitive operational information, such as production schedules, operating intensity, and business activities. Similar privacy concerns have been widely recognized in smart metering systems, where fine-grained electricity data can expose private behavioral and operational patterns [13]. Therefore, consumer-side carbon certification should not require enterprises to disclose raw load curves or detailed carbon emission records to all participants. Instead, the certification process should limit disclosure of sensitive enterprise-level data. Secret sharing and secure aggregation provide a feasible technical basis for this purpose, since private data can be split into multiple shares and reconstructed only under authorized conditions [14]. This motivates testing how masking and secret sharing affect both disclosure and accounting error.

To address the above challenges, this paper proposes a masked consumer-side carbon certification method for consumer-side carbon emissions based on clean electricity tracing. The proposed method first establishes a hydropower-based economic dispatch model to characterize the hourly clean electricity supply and system operation status. Based on the dispatch results, enterprise-side green electricity tracing is performed to determine the hourly clean electricity consumption of each enterprise, which is further converted into consumer-side carbon emission factors and carbon emissions. To protect sensitive enterprise electricity data, a privacy-preserving computation mechanism is incorporated into the certification process, enabling verifiable carbon certification without uploading unmasked clean-consumption records. The main contributions of this paper are summarized as follows.

1. A consumer-side carbon emission certification framework based on clean electricity tracing is proposed. The framework links hydropower-based economic dispatch, enterprise-side green

electricity tracing, carbon emission accounting, and trusted certification into a unified process.

2. An enterprise-level green electricity tracing and carbon accounting model is developed. By using hourly dispatch results, the proposed model calculates enterprise-specific clean electricity consumption, hourly carbon emission factors, and carbon emissions, thereby avoiding the temporal averaging problem of conventional emission factor methods.

3. A privacy-preserving carbon certification mechanism is designed. The mechanism supports carbon certification and verification without directly disclosing enterprise load curves or detailed carbon emission records, while allowing explicit evaluation of disclosure and error.

The Methods section presents the dispatch and privacy-preserving accounting models. Results are evaluated in a modified IEEE 39-bus system, followed by a discussion of the findings and limitations.

2 Results

2.1 Clean Electricity Tracing Results

Based on the system parameters and dispatch model established in Section 4.4, this section first presents the system-level power dispatch results, followed by network tracing using the proportional-sharing principle to analyze the impact of spatial location on nodal clean electricity ratios, and finally evaluates the differences in clean electricity consumption among enterprises with distinct industrial load characteristics. Fig. 1 illustrates the energy mix of the modified IEEE 39-bus system over a 24-hour dispatch horizon. As the primary clean energy resource, hydropower generation is driven by water balance constraints and dispatch requirements, exhibiting distinct time-varying characteristics. Based on the DCOPF power flow results, the real-time clean electricity ratio $\alpha_{i,t}$ for each node across the network is calculated using the proportional-sharing principle. Three representative nodes—Bus 31, Bus 39, and Bus 4—were selected for comparative analysis. As shown in Fig. 2, the availability of clean electricity across different nodes exhibits significant spatial heterogeneity:

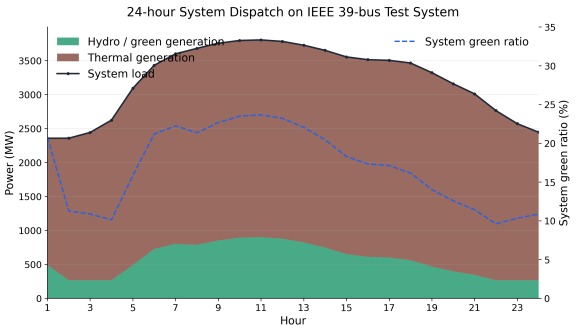


Fig. 1 24-hour system energy dispatch results (comparison of hydropower and thermal power output)

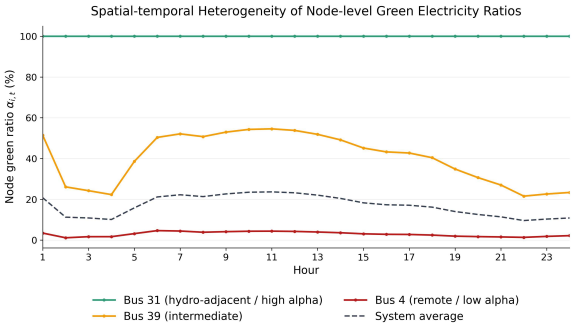


Fig. 2 24-hour clean electricity ratio profiles of representative nodes

- Bus 31: Located adjacent to the system's hydropower export center, this node achieves an average clean electricity ratio of approximately 100 percent, indicating that its load is almost entirely supplied by local or neighboring hydropower units.
- Bus 39: Situated along the intermediate transmission path, its average clean electricity ratio is approximately 40.18 percent. Influenced by a mix of thermal power injections and physical power flows, this node exhibits a moderate level of decarbonization.
- Bus 4: Acting as a remote load center, its average clean electricity ratio is only 2.95 percent. This demonstrates that, constrained by grid topology and power flow distribution, loads at the spatial periphery still heavily rely on thermal generation, despite the overall abundance of hydropower resources in the system.

These data strongly support the assertion that spatial location significantly impacts nodal clean electricity availability, demonstrating the

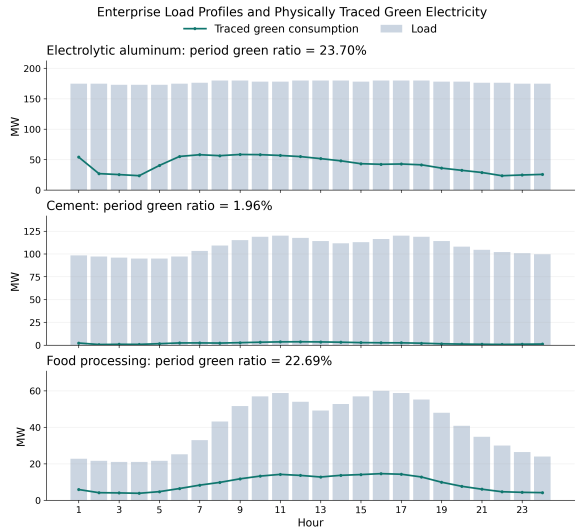


Fig. 3 Load profiles and clean electricity tracing results of three typical industrial enterprises

necessity of utilizing fine-grained, node-level tracing rather than system-average values for carbon emission accounting.

By further integrating the nodal clean electricity ratios with the load profiles of individual enterprises, the period-total clean electricity consumption ratio $\rho_e^{\mathrm{gr,per}}$ is calculated. Fig. 3 compares the load profiles of three typical industrial enterprises with their actually traced clean electricity consumption curves. Experimental results indicate substantial differences in the carbon mitigation performance of different enterprises:

- Aluminum-smelting enterprise: Due to the high continuity and stability of its load profile, it smoothly acquires clean electricity supply across all periods of the day, achieving a period-total clean electricity ratio of 23.70 percent.
- Food-processing enterprise: Exhibiting a distinct daytime double-peak characteristic that aligns well with the daytime fluctuations in system hydropower output, its clean electricity ratio reaches 22.69 percent.
- Cement enterprise: Because its load contains a substantial base component and its connection point may be located in an area with low clean electricity availability (e.g., near Bus 4), its period-total clean electricity ratio is only 1.96 percent.

In summary, the geographical location (nodal assignment) and the temporal consumption characteristics of an enterprise jointly determine its actual clean electricity consumption level. This establishes the physical foundation for conducting the subsequent differentiated, privacy-preserving carbon accounting.

2.2 Privacy-Preserving Enterprise Certification Results

To evaluate the effectiveness of the proposed privacy-preserving carbon accounting mechanism, this subsection compares the certification accuracy and privacy protection performance of different schemes. The food-processing enterprise, which exhibits significant hourly load fluctuations, is selected to visualize the single-process masking and reconstruction mechanism. Furthermore, statistical evaluations are conducted based on 100 Monte Carlo runs to quantify the error metrics.

Fig. 4 illustrates the time-series certification process for the food-processing enterprise under the proposed hybrid DP-SMPC scheme. A large fixed Gaussian mask μ_e is added to $G_{e,t}$ before upload. It conceals the absolute level of the uploaded series until threshold reconstruction, although differences between adjacent uploads cancel the fixed mask.

As shown in the inset of Fig. 4, the masked upload $\widetilde{G}_{e,t}$ shifts the series away from its true level; it does not remove its temporal shape. After the fixed mask is securely reconstructed and removed via the Shamir secret-sharing mechanism, the final released estimate $\widehat{G}_{e,t}$ tightly tracks the true consumption profile, with only the smaller hourly perturbation $\xi_{e,t}$ remaining. The reported experiments do not establish a formal differential-privacy guarantee for this released series.

To rigorously evaluate the accuracy of the released certification results, 100 Monte Carlo simulations were performed. The proposed hybrid scheme is compared against three baselines: the exact non-private scheme, the SMPC-only scheme, and the pure Local-DP scheme. The statistical error metrics, including MAE, RMSE, and period-total absolute error, are summarized in Table 1.

The hybrid scheme reduces absolute error relative to the local-DP baseline in this case study, while its non-zero percentage error and clipping rate remain material. Specifically, the hybrid DP-SMPC mechanism achieves an average MAE of 2.200 MW and an RMSE of 2.751 MW, which are

Table 1 Monte Carlo Error Metrics of Enterprise Green Electricity Certification

Scheme	MAE (MW)	RMSE (MW)	MAPE (%)	|Period error| (MWh)	Clipping rate (%)
Exact non-private	0.000	0.000	0.00	0.00	0.00
SMPC-only	0.000	0.000	0.00	0.00	0.00
Hybrid DP-SMPC	2.200	2.751	49.24	36.08	9.33
Local-DP	9.272	12.376	185.10	240.78	25.92

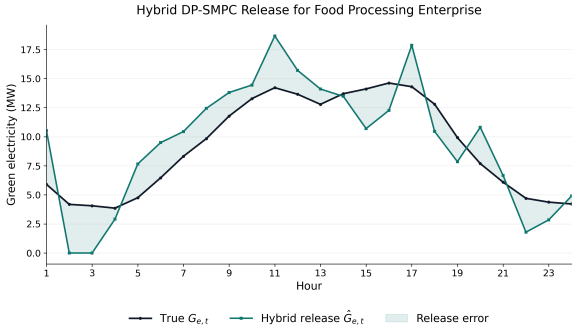


Fig. 4 Time-series certification results of the food-processing enterprise under the hybrid DP-SMPC scheme (Inset: the masked upload data with the fixed mask).

substantially lower than the 9.272 MW and 12.376 MW incurred by the Local-DP scheme.

This performance gap becomes even more pronounced when evaluating long-term carbon accounting accuracy. The period-total absolute error of the hybrid scheme is approximately 36.08 MWh, whereas the Local-DP scheme accumulates an error of about 240.78 MWh over the same horizon. The fixed mask is removed before release, so accuracy is governed mainly by the smaller hourly perturbation. The hybrid scheme still has a 49.24 percent MAPE and a 9.33 percent clipping rate; its privacy and utility should therefore be assessed for each intended use.

3 Discussion

Hourly clean electricity attribution differs substantially by node and enterprise in the modified IEEE 39-bus case. Bus-level clean electricity shares ranged from 2.95 to approximately 100 percent, and the three enterprises' period-total shares ranged from 1.96 to 23.70 percent. These differences show why a regional average factor can conceal spatial and temporal variation. The proposed tracing combines hydropower dispatch, network flows and enterprise load locations, but its proportional-sharing allocation is a model-based attribution rather than a direct measurement of individual electrons.

The hybrid certification scheme reduced mean absolute error from 9.272 MW for local DP to 2.200 MW in 100 Monte Carlo runs; its period-total absolute error fell from 240.78 to 36.08 MWh. The method masks uploads before reconstruction, but repeated use of a fixed mask preserves relative hourly changes, and removal of that mask leaves the released sequence protected only by the smaller perturbation. Because the study does not specify a privacy budget or prove a composition bound, these results establish an accuracy comparison under the stated noise settings, not a formal differential-privacy guarantee. The 49.24 percent MAPE and 9.33 percent clipping rate also limit claims of universally accurate certification.

The model considers hydropower as its only clean resource, uses one modified network and three constructed enterprise profiles, and omits cross-regional trading. Evaluation with wind and solar generation, measured enterprise loads, independent networks and explicit privacy accounting is needed before operational deployment.

4 Methods

4.1 Hydropower dispatch

The 24-hour dispatch minimizes thermal generation cost; hydropower is treated as dispatchable clean generation without an explicit water opportunity cost [15, 16]. For thermal units g, hydropower units h, buses i and hours t, the objective and energy balance are

$$\begin{aligned} &\min \sum_{t,g} \left[a_g (P^{\mathrm{th}}_{g,t})^2 + b_g P^{\mathrm{th}}_{g,t} + c_g \right] \Delta t, \\ &\sum_{g} P^{\mathrm{th}}_{g,t} + \sum_{h} P^{\mathrm{hy}}_{h,t} = \sum_{i} D_{i,t}. \end{aligned} \tag{1}$$

Generation is bounded by the unit-specific limits in Table 2. Thermal ramping uses the stated initial output $P^{\mathrm{th}}_{g,0} = P^{0}_{g}$; hydropower ramping applies

from the second hour:

$$\begin{aligned} P_g^{\min,\mathrm{th}} \le P_{g,t}^{\mathrm{th}} \le P_g^{\max,\mathrm{th}}, \\ -RD_g^{\mathrm{th}}\Delta t \le P_{g,t}^{\mathrm{th}} - P_{g,t-1}^{\mathrm{th}} \le RU_g^{\mathrm{th}}\Delta t, \\ P_h^{\min,\mathrm{hy}} \le P_{h,t}^{\mathrm{hy}} \le P_h^{\max,\mathrm{hy}}, \\ -RD_h^{\mathrm{hy}}\Delta t \le P_{h,t}^{\mathrm{hy}} - P_{h,t-1}^{\mathrm{hy}} \le RU_h^{\mathrm{hy}}\Delta t \quad (t>1). \end{aligned} \tag{2}$$

Reservoir operation follows water balance with $V_{h,0} = V_h^0$ and natural inflow $I_{h,t}$ [17, 18]. Discharge $Q_{h,t}$, spillage $S_{h,t}$, storage $V_{h,t}$ and terminal storage remain within their unit-specific limits:

$$\begin{aligned} V_{h,t} = V_{h,t-1} + (I_{h,t} - Q_{h,t} - S_{h,t})\Delta t, \\ P_{h,t}^{\mathrm{hy}} = \eta_h Q_{h,t}, \quad V_h^{\min} \le V_{h,t} \le V_h^{\max}, \\ Q_h^{\min} \le Q_{h,t} \le Q_h^{\max}, \quad 0 \le S_{h,t} \le S_h^{\max}, \\ V_h^{\min,\mathrm{end}} \le V_{h,T} \le V_h^{\max,\mathrm{end}}. \end{aligned} \tag{3}$$

Network flows are obtained from bus injections using a DC power-transfer distribution factor (PTDF) matrix. Local generation sets are denoted by $\mathcal{G}_i^{\mathrm{th}}$ and $\mathcal{G}_i^{\mathrm{hy}}$:

$$\begin{aligned} p_{i,t}^{\mathrm{inj}} = \sum_{g\in\mathcal{G}_i^{\mathrm{th}}} P_{g,t}^{\mathrm{th}} + \sum_{h\in\mathcal{G}_i^{\mathrm{hy}}} P_{h,t}^{\mathrm{hy}} - D_{i,t}, \\ f_{l,t} = \sum_i H_{l,i} p_{i,t}^{\mathrm{inj}}, \qquad |f_{l,t}| \le F_l^{\max}. \end{aligned} \tag{4}$$

These constraints determine the hourly hydropower output and directed power flows used in tracing.

4.2 Enterprise clean electricity tracing

The proportional-sharing model assigns the same electricity mix to a bus's outgoing flows and local demand [7, 19, 20]. For an oriented branch $l : i \to j$, define $F_{ij,t}^+ = \max(f_{l,t}, 0)$ and $F_{ji,t}^+ = \max(-f_{l,t}, 0)$. Hydropower is the clean source in this case; thus $G_{i,t}^{\mathrm{gr}} = \sum_{h\in\mathcal{G}_i^{\mathrm{hy}}} P_{h,t}^{\mathrm{hy}}$. The clean fraction $\alpha_{i,t}$ solves

$$\alpha_{i,t}\left(D_{i,t} + \sum_j F_{ij,t}^+\right) - \sum_j \alpha_{j,t} F_{ji,t}^+ = G_{i,t}^{\mathrm{gr}}. \tag{5}$$

For each hour, Eq. (5) is a linear system $\boldsymbol{A}_t\boldsymbol{\alpha}_t = \boldsymbol{b}_t$, with $A_{t,ii} = D_{i,t} + \sum_j F_{ij,t}^+$, $A_{t,ij} = -F_{ji,t}^+$ for $i \ne j$, and $b_{t,i} = G_{i,t}^{\mathrm{gr}}$. The resulting fraction is bounded to $[0, 1]$. Enterprise load $L_{e,i,t}$ is consistent with nodal demand through $D_{i,t} = \sum_{e\in\mathcal{E}_i} L_{e,i,t} + L_{i,t}^{\mathrm{oth}}$. The enterprise's load, clean electricity, and clean fraction are

$$\begin{aligned} L_{e,t} = \sum_{i\in\mathcal{B}_e} L_{e,i,t}, \qquad G_{e,t} = \sum_{i\in\mathcal{B}_e} \alpha_{i,t} L_{e,i,t}, \\ \rho_{e,t}^{\mathrm{gr}} = G_{e,t}/L_{e,t}, \qquad \rho_e^{\mathrm{gr,per}} = \frac{\sum_t G_{e,t}\Delta t}{\sum_t L_{e,t}\Delta t}. \end{aligned} \tag{6}$$

With clean and non-clean emission factors κ^{gr} and κ^{ng}, hourly emissions and the period total are

$$\begin{aligned} C_{e,t} = [\kappa^{\mathrm{gr}} G_{e,t} + \kappa^{\mathrm{ng}}(L_{e,t} - G_{e,t})]\Delta t, \\ C_e^{\mathrm{per}} = \sum_t C_{e,t}. \end{aligned} \tag{7}$$

The study sets $\kappa^{\mathrm{gr}} = 0$ for emissions during electricity use.

4.3 Masked certification and evaluation

To avoid sending raw $G_{e,t}$, each enterprise draws a fixed mask $\mu_e \sim \mathcal{N}(0, \sigma_{\mathrm{fix}}^2)$ and an hourly perturbation $\xi_{e,t} \sim \mathcal{N}(0, \sigma_{\mathrm{small}}^2)$. The fixed mask is shared with K trustees through a degree-$(\tau-1)$ Shamir polynomial $\phi_e(x) = \mu_e + \sum_{q=1}^{\tau-1} a_{e,q} x^q$; trustee k receives $s_{e,k} = \phi_e(k)$ [14]. Any τ shares reconstruct the mask by Lagrange interpolation:

$$\widehat{\mu}_e = \sum_{k\in\mathcal{K}_\tau} s_{e,k} \prod_{\substack{r\in\mathcal{K}_\tau \\ r\ne k}} \frac{-r}{k-r} = \mu_e. \tag{8}$$

The enterprise uploads $\widetilde{G}_{e,t} = G_{e,t} + \mu_e + \xi_{e,t}$. After reconstructing and removing the fixed mask, the released quantity is bounded by the observed load:

$$\begin{aligned} \widehat{G}_{e,t}^{\mathrm{raw}} = \widetilde{G}_{e,t} - \widehat{\mu}_e = G_{e,t} + \xi_{e,t}, \\ \widehat{G}_{e,t} = \min\{L_{e,t}, \max\{0, \widehat{G}_{e,t}^{\mathrm{raw}}\}\}. \end{aligned} \tag{9}$$

Certified ratios and emissions follow Eqs. (6) and (7) after replacing $G_{e,t}$ by $\widehat{G}_{e,t}$. Before clipping, $\widehat{G}_{e,t}^{\mathrm{raw}}$ has mean $G_{e,t}$ and variance $\sigma_{\mathrm{small}}^2$; clipping can introduce bias. We assess hourly

mean absolute error (MAE), root mean square error (RMSE), mean absolute percentage error (MAPE), period-total absolute error, and clipping frequency over 100 Monte Carlo runs. The fixed mask protects the upload before reconstruction; because it is subsequently removed, the released sequence retains only the smaller hourly perturbation. No formal differential-privacy budget is claimed for that final sequence.

4.4 Case-study design

To evaluate the proposed privacy-preserving consumer-side certification method, case studies are conducted on a modified IEEE 39-bus system. The hydropower-based economic dispatch model is implemented in PYOMO/PYTHON and solved using Gurobi. The dispatch interval is set to $\Delta t = 1$ h, and the system load profile is adapted from the Open Power System Data time-series package [21]. The parameters and cost coefficients of thermal units are adapted from [15, 22, 23]. Hydropower is regarded as the clean generation resource in the tracing model, and clean electricity is treated as zero-carbon electricity during the use stage, i.e., $\kappa^{\mathrm{gr}} = 0$. The hydropower-related settings, including reservoir storage limits, initial storage, terminal storage requirements, discharge limits, spillage limits, inflow profiles, and water-to-power conversion efficiency, are configured based on hydrothermal scheduling studies, reservoir-operation references, and hydropower operation guidelines [17, 18, 24–27]. The main generation-side parameters are summarized in Table 2, and the enterprise-level load and location settings are summarized in Table 3. These settings enable the dispatch model to capture the inter-temporal water balance and physical operating limits of hydropower units before the resulting clean generation and network flow results are used for electricity tracing.

For enterprise-side certification, three representative industrial consumers are considered: an aluminum-smelting enterprise with a continuous and stable load profile, a cement enterprise with continuous base demand and shiftable production components, and a food-processing enterprise with a daytime double-peak load profile. The enterprise load profiles are constructed with reference to electricity-demand curve studies and industrial-load modeling literature [28–30]. In the privacy-preserving certification experiments, the fixed-mask standard deviation, small perturbation standard deviation, and local-DP noise standard deviation are set to $\sigma_{\mathrm{fix}} = 80$, $\sigma_{\mathrm{small}} = 3$, and $\sigma_{\mathrm{local}} = 15$, respectively. The number of trustees is set to $\mathrm{K} = 5$, the reconstruction threshold is set to $\tau = 3$, and each randomized experiment is repeated 100 times for Monte Carlo evaluation. Four certification schemes are compared: an exact non-private scheme, an SMPC-only scheme, the proposed hybrid DP-SMPC scheme, and a local-DP scheme. The exact non-private scheme serves as the accuracy benchmark, the SMPC-only scheme represents exact secure aggregation without perturbation, and the local-DP scheme provides a direct perturbation-based privacy-preserving baseline.

Data availability

The datasets generated and analysed during the current study, including the modified IEEE 39-bus system parameters, constructed enterprise load profiles, and simulation results, are available from the corresponding author upon reasonable request.

Acknowledgements

This research is supported by the Science and Technology Project of Sichuan Electric Power Company (No. 52199725000S).

Author contributions

Lingyu Chen: Conceptualization, Methodology, Software, Formal analysis, Investigation, Data curation, Visualization, Writing–original draft, Writing–review & editing.
Yang Wei: Methodology, Validation, Formal analysis, Writing–review & editing.
Xiangxi Duan: Resources, Project administration, Writing–review & editing.
Hongli Liu: Investigation, Data curation, Validation.
Han Zhang: Software, Investigation, Visualization.
Yumin Chen: Resources, Validation, Writing–review & editing.
Junhua Zhao: Conceptualization, Supervision, Writing–review & editing.

Table 2 Generation and hydropower-reservoir settings

Panel A: Thermal unit settings

Unit	Bus	$P^{\min}$ (MW)	$P^{\max}$ (MW)	RU (MW/h)	RD (MW/h)	P^{0} (MW)	a_g	b_g	c_g
4	33	180	652	90	90	360	0.0085	34	250
5	34	150	508	70	70	280	0.0115	72	900
6	35	210	687	95	95	390	0.0135	88	1400
7	36	175	580	80	80	310	0.0115	72	900
8	37	140	564	80	80	260	0.0065	38	350

Panel B: Hydropower and reservoir settings

Unit	Bus	$P^{\min}$	$P^{\max}$	RU/RD	$V^{\min}$	$V^{\max}$	V^{0}	$V^{\min,\text{end}}$	$V^{\max,\text{end}}$	$Q^{\min}$	$Q^{\max}$	η_h
10	30	45	180	120/120	2500	12000	8500	7000	12000	55.00	220	0.8182
2	31	45	180	120/120	2500	12000	8500	7000	12000	55.00	220	0.8182
3	32	70	260	150/150	3000	15000	10500	8500	15000	86.15	320	0.8182
9	38	60	220	140/140	2800	14000	9800	7800	14000	81.82	300	0.7333
1	39	45	180	120/120	2500	12000	8500	7000	12000	55.00	220	0.8182

Note: The maximum spillage $S^{\max}$ is 250, 250, 360, 340, and 250 for hydropower units 10, 2, 3, 9, and 1, respectively. The hourly inflow is set to 65, 65, 85, 75, and 65 for the corresponding units.

Table 3 Enterprise load and location settings

Enterprise	Buses	$\overline{L}_e$ (MW)	$L_e^{\max}$ (MW)	$L_e^{\min}$ (MW)	L_e^{per} (MWh)	Load type
Aluminum-smelting	39, 20, 8, 4	177.15	180.00	172.80	4251.60	Stable
Cement	16, 3, 15	107.70	120.00	94.80	2584.80	Base + shiftable
Food-processing	24, 29, 27	40.32	60.00	21.00	967.80	Double-peak

Note: $\overline{L}_e$, $L_e^{\max}$, $L_e^{\min}$, and L_e^{per} denote the average load, peak load, minimum load, and daily electricity consumption of enterprise e, respectively. The complete hourly profiles are shown in Fig. 3.

Tianze Yu: Methodology, Supervision, Writing–review & editing.

All authors reviewed and approved the final manuscript.

Competing interests

The authors declare no competing interests.

References

[1] International Sustainability Standards Board. IFRS S2 climate-related disclosures. Tech. Rep., IFRS Foundation (2023). Accessed 24 April 2026.

[2] International Energy Agency. Electricity 2024. Tech. Rep., International Energy Agency, Paris, France (2024). Accessed 24 April 2026.

[3] Greenhouse Gas Protocol. GHG Protocol Scope 2 Guidance: An amendment to the GHG Protocol Corporate Standard. Tech. Rep., World Resources Institute (2015). Accessed 24 April 2026.

[4] Miller, G. J., Novan, K. & Jenn, A. Hourly accounting of carbon emissions from electricity consumption. *Environmental Research Letters* **17**, 044073 (2022).

[5] UN-Energy. 24/7 carbon-free energy compact (2021). URL https://www.un.org/en/energy-compacts/page/compact-247-carbon-free-energy. Accessed 24 April 2026.

[6] Liu, X. *et al.* A review of main carbon accounting methods for thermal power plants under the dual-carbon goals. *Sichuan Electric Power Technology* **47**, 34–43 (2024).

[7] Bialek, J. Tracing the flow of electricity. *IEE Proceedings-Generation, Transmission and Distribution* **143**, 313–320 (1996).

[8] Kang, C. *et al.* Carbon emission flow in networks. *Scientific Reports* **2**, 479 (2012).

[9] Scholta, H. F. & Blaschke, M. J. Temporal matching as an accounting principle for green electricity claims. *Nature Communications*

16, 9280 (2025).

[10] Riepin, I. & Brown, T. On the means, costs, and system-level impacts of 24/7 carbon-free energy procurement. *Energy Strategy Reviews* **54**, 101488 (2024).

[11] International Energy Agency. Hydropower special market report: Analysis and forecast to 2030. Tech. Rep., OECD Publishing (2021).

[12] Huertas-Hernando, D. *et al.* Hydropower flexibility for power systems with variable renewable energy sources: An iea task 25 collaboration. Advances in Energy Systems: The Large-Scale Renewable Energy Integration Challenge (2019).

[13] Asghar, M. R., Dán, G., Miorandi, D. & Chlamtac, I. Smart meter data privacy: A survey. *IEEE Communications Surveys & Tutorials* **19**, 2820–2835 (2017).

[14] Shamir, A. How to share a secret. *Communications of the ACM* **22**, 612–613 (1979).

[15] Liao, H. *et al.* Comprehensive-contribution-based primary frequency regulation market design for the converter-integrated power system. *IEEE Transactions on Power Systems* **39**, 3825–3838 (2023).

[16] Wu, F., Xu, C., Luo, W., Ye, L. & Lei, X. A CVaR-based short-term scheduling model for cascade hydropower plants and its linearization. *Sichuan Electric Power Technology* **48**, 54–62 (2025).

[17] Yan, H., Luh, P. B., Guan, X. & Rogan, P. M. Scheduling of hydrothermal power systems. *IEEE Transactions on Power Systems* **8**, 1358–1365 (2002).

[18] Nilsson, O. & Sjelvgren, D. Mixed-integer programming applied to short-term planning of a hydro-thermal system. *IEEE Transactions on Power Systems* **11**, 281–286 (2002).

[19] Kirschen, D., Allan, R. & Strbac, G. Contributions of individual generators to loads and flows. *IEEE Transactions on Power Systems* **12**, 52–60 (2002).

[20] Kang, C. *et al.* Carbon emission flow from generation to demand: A network-based model. *IEEE Transactions on Smart Grid* **6**, 2386–2394 (2015).

[21] Open Power System Data. Time series data package (version 2020-10-06) (2020). URL https://data.open-power-system-data.org/time_series/2020-10-06/. Dataset accessed 4 June 2025.

[22] Morren, J., Pierik, J. & Haan, S. W. D. Inertial response of variable speed wind turbines. *Electric Power Systems Research* **76**, 980–987 (2006).

[23] Soroudi, A. *Power System Optimization Modeling in GAMS* Vol. 78 (Springer, 2017).

[24] U.S. Army Corps of Engineers Hydrologic Engineering Center. Reservoir operations—the basics. URL https://www.hec.usace.army.mil/confluence/ResSimDocs/rsum/reservoir-operations/reservoir-operations-the-basics. HEC-ResSim User's Manual; accessed 24 April 2026.

[25] l. Ge, X., z. Zhang, L., Shu, J. & f. Xu, N. Short-term hydropower optimal scheduling considering the optimization of water time delay. *Electric Power Systems Research* **110**, 188–197 (2014).

[26] U.S. Bureau of Reclamation. Hydroelectric power: How it works. URL https://www.usbr.gov/power/edu/pamphlet.pdf. Accessed 24 April 2026.

[27] Pavlov, V. Spillway design guide. Tech. Rep. FRS20238/R12, Environment Agency (2022). URL https://assets.publishing.service.gov.uk/media/62b32702d3bf7f0afc388104/Spillway_Design_Guide_1.pdf.

[28] Castillo, V. Z. *et al.* Future global electricity demand load curves. *Energy* **258**, 124741 (2022).

[29] Al-Odat, M., Al-Hasan, M., Obeidat, F. & Chamkha, A. J. Optimization of on-grid hybrid PV/wind system for a cement factory in kuwait using HOMER Pro software. *International Journal of Low-Carbon Technologies* **19**, 120–126 (2024).

[30] Yao, M., Hu, Z., Sifuentes, F. & Zhang, N. Integrated power management of conventional units and industrial loads in china's ancillary services scheduling. *Energies* **8**, 3955–3977 (2015).